

DETAILED COMPOSITIONAL ANALYSIS

The detailed compositional analysis of ODC particles utilized Scanning Electron Microscope (SEM) methods combined with Energy Dispersive X-Ray Spectroscopy (EDS). These techniques were first applied to space-exposed surfaces of the Solar Maximum satellite (Warren *et al.*, 1989), and became routine in the analyses of LDEF surfaces (Levine, 1991; 1992; 1993). They are also the method of choice for the continued monitoring and evaluation of impact features on Shuttle surfaces (Christiansen *et al.*, 1998). The major difference between these earlier studies and the ongoing ODC work relates to the availability of numerous, essentially unmelted particle fragments, whereas previous studies were largely confined to the analysis of molten impactors. The analyses presented in this section are merely examples of representative particle types to support some of the descriptions and interpretations offered and to illustrate the potential of the SEM-EDS technique(s). In addition, these examples illustrate the significant level of effort needed for any systematic, statistically meaningful assessment of the particle populations captured by ODC.

Sample Recovery and Preparation

Although the SEM-EDS methods are fairly routine, substantial new efforts went into the development of suitable methods to recover the particle residue from its friable aerogel matrix, and to design suitable sample preparation procedures for the contemplated SEM studies. Major emphasis was placed on minimizing the loss of samples, commonly < 10 μm in size, as well as on avoiding contamination, both chemical and particulate, during all extraction and sample preparation steps. Most sample extractions are carried out in a Class 1000 flow bench, housed inside the FOILS laboratory. Individual aerogel tiles are readily split via a razorblade into sub-samples on the order of 1 cm^2 in surface, with each sub-sample typically containing a single track. The actual impact feature of interest and its particle is then photographically documented, both in plan and side view with the CCD camera system or via optical (Polaroid) photography, or both. Following photo-documentation, individual tracks are physically split with a razor blade, generally under a binocular microscope. The track represents a substantial flaw on the scale of the centimeter-sized aerogel samples, the reason why the material fails along the actual track when applying highly localized pressure via the razor blade. Typically, the aerogel is not cut, but cleaves into two halves during such operations. Obviously, this aerogel splitting is not perfect and most of the terminal residue is confined to one half, commonly buried under a thin layer of aerogel. The aerogel-covered residue is then removed from the tile sample by utilizing a single-bristle brush. If only small masses of aerogel adhere to the extracted particle, the sample may be transferred directly to a graphite SEM planchette. However, typically the material is transferred to a petri dish for removal of excess aerogel until substantial surface fractions of the residue are exposed for direct electron beam exposure. On rare occasions, particle residue may be exposed immediately after the track-splitting procedure, in which case the entire track and its particle are transferred to a planchette. This procedure works well for tracks as small as 1 mm, yet we do not know whether it is suitable for still smaller tracks. The most critical steps are the actual track splitting and the quarrying operations to dislodge materials from the halved terminus. Both result in small samples that tend to charge electrostatically and that are difficult to steady. Electrostatic charging of small, transparent, and difficult to see volumes of aerogel is the major reason for

sample loss. Charging, specimen movement and potential sample loss may even occur during electron-beam radiation inside the SEM's vacuum chamber, because small samples of aerogel are simply difficult to attach and secure to any surface.

Representative Results

Consistent with the above morphologic descriptions of impact features, we offer the following representative examples of shallow depressions, pits, and slender tracks. The detailed documentation for individual particles typically consists of optical images in plan view and cross section, an SEM image, and an EDS spectrum of the recovered residue. In addition, we include Transmission Electron Microscope (TEM) images of an unmelted natural cosmic-dust particle recovered in LEO.

Man-Made Particles - The liquid-droplet feature introduced in Figure 29 is again seen in Figure 41. With the impactor residue already exposed in the bottom of the feature, little sample processing was required for detailed SEM investigations. The plan view image focuses on the bottom of the feature and the evaporite deposit. Other circular elements, such as the entrance hole, are out of focus and merely hinted by partial arcs of reflected light. Note the structurally complex, yet highly circular nature of the cavity. An SEM image is presented in the lower left and illustrates the entrance hole and a shoulder formed by a peculiar cavity restriction at depth (see cross section). This image also demonstrates the absence of any fracturing and mechanical damage, corroborating our earlier conclusion that such features result from the interaction of aerogel with some liquid, and that they are solution pits and not the products of mechanical displacement. The EDS spectrum of the evaporite deposit reveals the biogenic elements Cl, S, K, and Na; the Si peak is derived from the aerogel substrate. Specifically, the substantial quantities of Cl and S provide the most diagnostic criterion for human waste. Essentially identical spectra were obtained on all ODC droplet-type features analyzed to date, as well as on the evaporite deposits on the companion PPMD and POSA MEEP experiments (Kinard, 1998; Pippin, 1998). There seems little doubt that these features result from Shuttle operations, which currently call for the dumping ~ 20 gallons of waste water every three days.

Figure 42 shows the large flake impact first illustrated in Figure 27. This particle clearly broke up during impact, and large, irregular, platy fragments adhere to the bottom of a rather shallow depression. The latter mimics the irregular projectile shape in outline. These morphologic characteristics are typical for all flake impacts and they are in stark contrast to the liquid-droplet pits shown in Figure 41. Nevertheless, the EDS spectrum of the flake fragments is largely composed of biogenic elements (*e.g.*, Na, P, and S). Unlike the previous example, the sample thickness exceeds the X-ray excitation depth, so that substantial parts, if not all, of the Si peak must be derived from the flake particle itself. The lack of Cl seems highly significant for human-waste products; additional ODC examples that contain no Cl, could be shown, suggesting a previously unrecognized particle type in the ODC aerogel. However, some flake residues do contain Cl, akin to Figure 41. Cl-bearing materials were frequently observed on LDEF, as well as most other space-exposed surface, and are typical for human waste. Such Cl-deficient spectra appear consistent with pure soap, yet we do not know of any specific mechanism that would preserve pure soap particles in Cl-containing wastewater. The source and origin of these Cl-deficient particles is currently unclear.

Human Waste

1C01-8

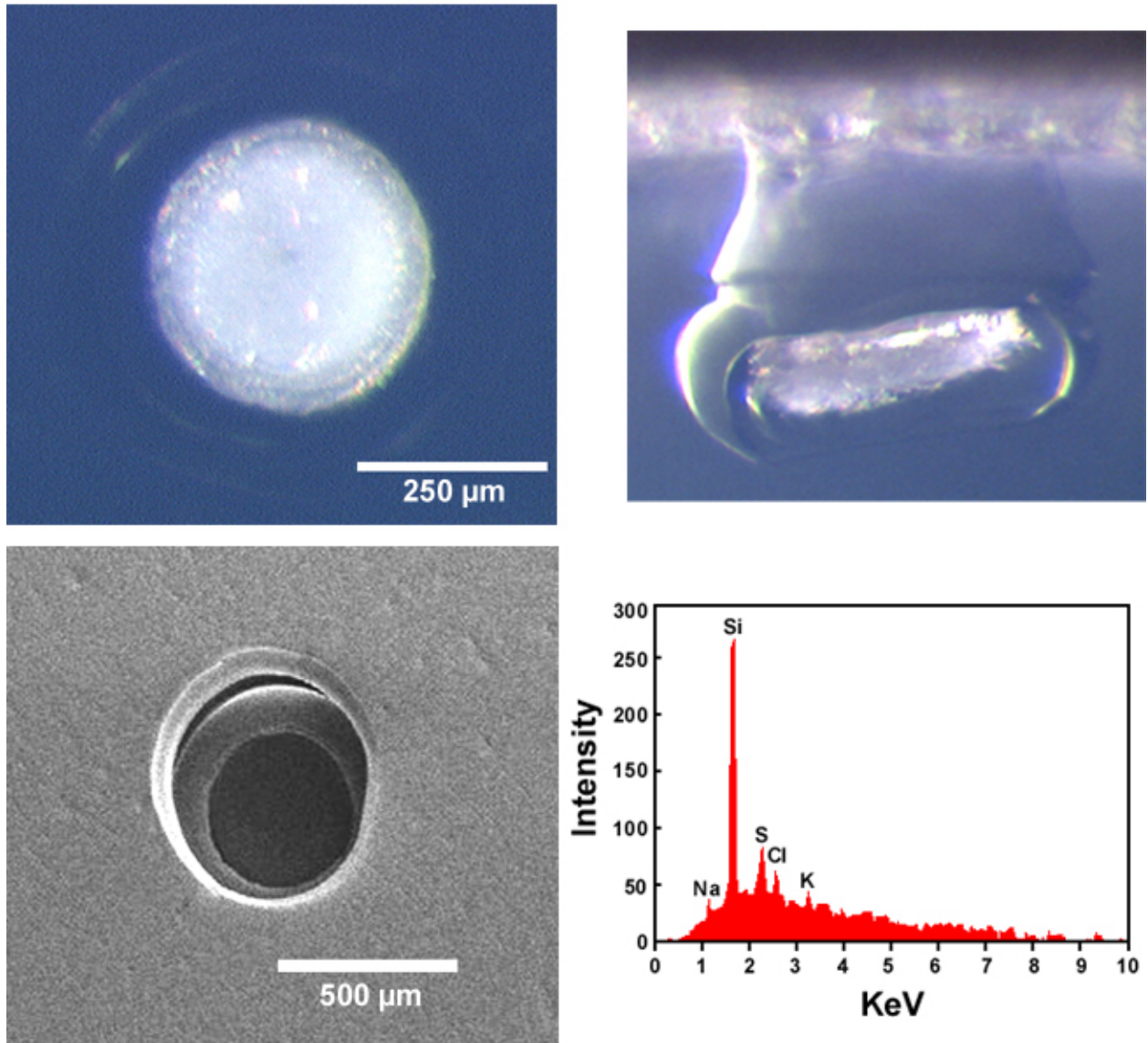


Figure 41. Example of the detailed analysis of an individual droplet feature, including SEM imaging and EDS techniques. Note the substantial depth of this feature, its smooth outlines, and the total lack of any mechanically deformed and micro-fractured aerogel. Typically, these structures have an opening at the surface of the aerogel that is narrower than the bottom of the feature. The "projectile" residue is confined to a lens of smaller radius than the bulbous cavity (partial outline visible in top-left plan view). The presence of biogenic elements (*i.e.*, Na, S, Cl & K) can be seen in the X-ray spectrum; the Si peak is largely caused by the Si-based aerogel substrate.

Flake Particle 1C01-07

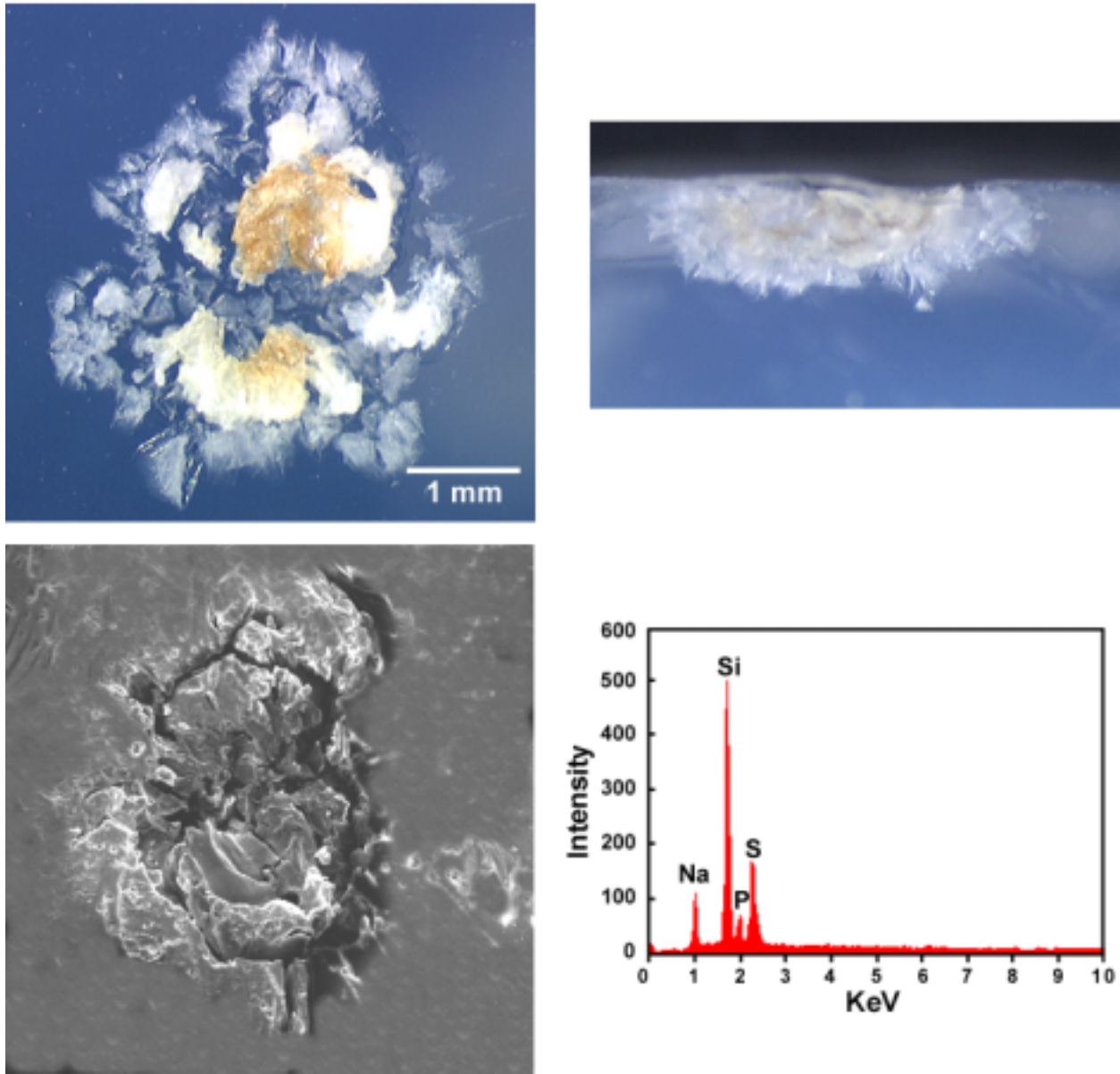


Figure 42. Large flake feature previously shown in Figure 29. Note the EDS spectrum contains no Cl, yet it is dominated by the biogenic elements Na, P, and S.

The terminal sections of a typical, carrot-shaped penetration track and its associated residue are illustrated in plan view and cross section in Figure 43; the aerogel surface illustrated in the cross section is not the original tile surface, but a razorblade induced fracture. Note the well-developed cone-in-cone structure and the misalignment of the last few cones, causing the track to curve and the particle to reside off the true axis of the track. The residue is the largest particle

recovered from ODC to date, $\sim 200 \mu\text{m}$ across. Also note its jagged, sharp corners and what appears to be mechanical striation and abrasion on the particle's surface, both observations arguing against pervasive melting. The EDS spectrum of this particle is dominated by Ti and Zn, which constitute the pigments of many thermal protective paints. Similar particles/spectra are known from most other space-exposed surface; thermal protective paints are prone to substantial abrasion by small-scale impacts, and their largely organic binders degrade when exposed to atomic oxygen and/or UV.

In addition to the two examples shown, we recovered and analyzed ~ 20 residues from ODC that must be classified as man-made debris. These include particles rich in Fe, with subordinate levels of Ni and/or Cr, the latter characteristic of stainless steel. In addition, Cu-rich particles reflect fragments of electronic compounds, some even associated with Ag from silver solders. Unlike LDEF, however, particles dominated by Al seem rare on ODC. Two examples of essentially pure metallic aluminum were found that represent structurally disintegrated components, while only a single Al_2O_3 particle was discovered so far. Clearly, more particles need to be analyzed in order to arrive at statistically firm conclusions, or before some significant difference with LDEF can be established.

A relatively large fraction ($\sim 90\%$) of all impactors can be classified into man-made or natural-particle categories. Figure 44 represents one of the ambiguous cases. This spectrum was taken with a thin beryllium window that allows analysis of oxygen, thus the significant oxygen signal; the C peak represents carbon-coat to make the particle's surface electrically conductive, while the Si is likely derived from aerogel adhering to the particle. This identifies this particle as being essentially pure iron oxide, without specifying the exact stoichiometry. It could be natural, such as isolated crystals of hematite (Fe_2O_3) or magnetite (Fe_3O_4), known to occur in meteorites, or it could be man-made iron that was oxidized (*e.g.*, during explosive or impact-derived origins). The lack of any alloying component, such as Cr, W, or Ni argues against most popular steels and leads us to prefer a natural source. Nevertheless, the origin of this particle remains ambiguous. In the cross-section image, note that considerable mass was shed from the projectile and deposited along much of the stylus. The recovered residue appears deformed, if not molten. Its maximum diameter (D_p) is $\sim 10 \mu\text{m}$, which compares to a total track length of $\sim 1,400 \mu\text{m}$, resulting in a $D_p/L = 140$ for this relatively dense impactor. Such D_p/L values are typical for tracks produced at light-gas gun velocities of 4 to 7 km/s (Hörz *et al.*, 1997) using less-dense glass projectiles.

Paint Flake

1A06-17

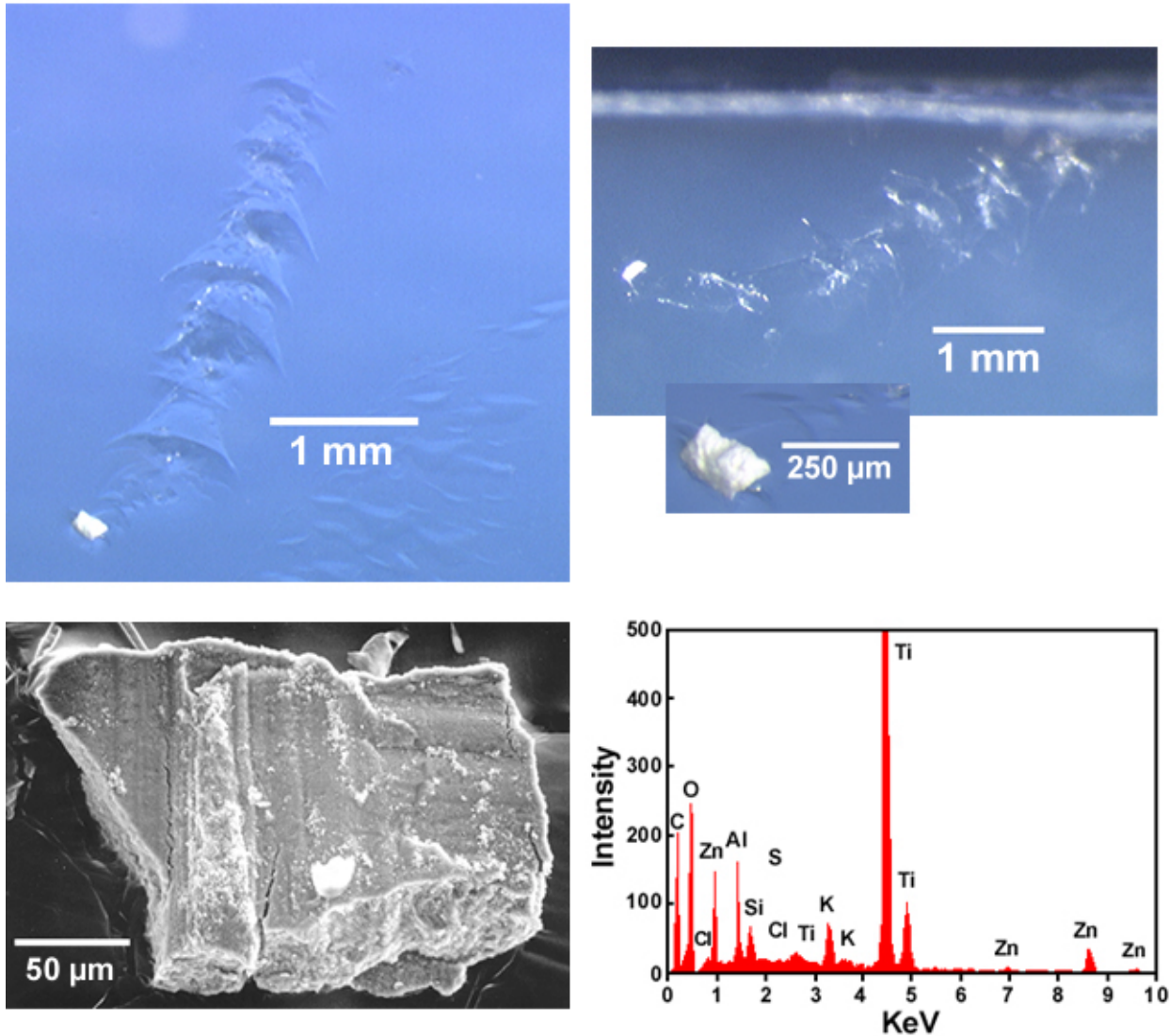


Figure 43. Detailed analysis of a man-made particle. Note the cone-in-cone structure and the misalignment of the last few cones with the overall track axis. The recovered particle exhibits a highly irregular, if not jagged and sharp-edged surface, suggesting that very little rounding, much less melting, occurred during the capture process. The dominance of Ti and Zn identifies this particle as paint (pigments), with other elements being part of the organic binder.

Fe Oxide Particle

1C01-13

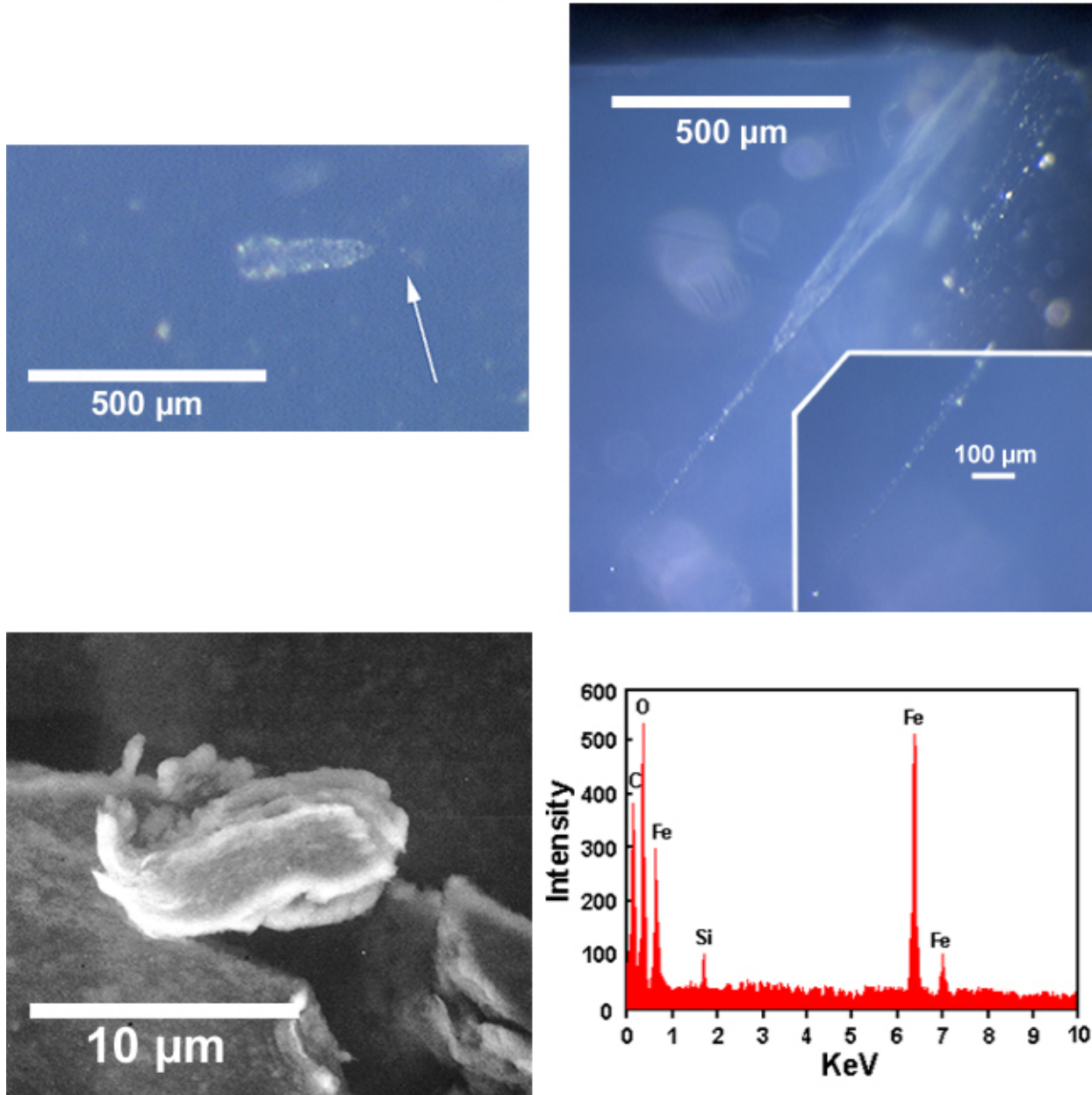


Figure 44. Example of a particle, ~ 10 μm in length, that resided at the terminus of a 1.2 mm long track. Note the shedding of light-colored projectile material along the stylus. This particle appears to have been either plastically deformed or molten during capture process. Compositionally, it is Fe-oxide and could either be man-made or natural in origin.

Natural Impactors - The residue, ~ 12 μm in diameter, recovered from an ~ 1 mm long swarm track (left track in optical image) is illustrated in Figure 45. As is common for natural particles, they tend to be composed of very fine-grained aggregates of sub-micron sized components which in turn leads to modestly variable distributions of the dominant elements, Mg, Ca, and Fe, and substantial variations in minor elements, such as Al, S, or Ni. Nevertheless, most any analysis spot would identify such compositions as *chondritic* in nature and of natural origin (e.g., Brownlee, 1986; Zolensky *et al.*, 1994). Another 1.2 mm long swarm track that yielded a particle ~ 5 μm across can be seen in Figures 46. Note the similarity of the spectrum to that of Figure 45. An additional 5 residues recovered from swarm tracks are of similar make up, identifying the swarm to be composed of fragments from a natural impactor. While this is not a surprising result, the preponderance of projectile fragments only composing the debris swarm is somewhat surprising, as one would expect to find fragments of the target as well. In fact, target fragments should dominate, as hypervelocity impactors readily excavate and displace 10 to 100 times their own mass. The current observation that projectile fragments make up the swarm calls for unusual conditions for the primary impact. One scenario is that of a very shallow incidence impact, which lead to the decapitation of the impactor and a fragment cloud that is dominated by or exclusively composed of projectile species (e.g., Schultz and Gault, 1990). Alternatively, the impactor may have fragmented upon penetration of a thin film on Mir, such as a thermal insulation blanket, resulting in a debris plume that is utterly dominated by projectile fragments (e.g., Hörz *et al.*, 1995). Additional analyses of swarm tracks are warranted to possibly identify the target-material.

Natural impactors, unrelated to the swarm event, are shown in Figures 47 and 48. The large grain (30 μm) recovered from track 2D03-23 is documented in Figure 47. SEM and TEM analysis determined this projectile is micrometeoritic in origin. In Figure 48, the track split such that parts of the residue surface were exposed, permitting SEM imaging of the particle in-situ. As is commonly observed, a substantial volume of molten aerogel drapes the entire particle. The EDS spectrum reveals the presence of mafic silicates (Fe, Mg, and Si) and most likely the presence of a K-rich feldspar (Al and K). Following these SEM analysis, the particle was embedded in epoxy and thin-sectioned into 1000 \AA thick slices with a microtome for more detailed mineralogical investigations by Transmission Electron Microscopy (TEM) as illustrated in the two bottom panels and as described by Hörz *et al.* (1998). The TEM investigations reveal significant disruption of the parent grain by invading aerogel melt, the presence of hydrated layer-lattice silicates (grey material), and small (sub-micron) oxide grains (dark material); the arrow points to the magnified particle visible in the bottom, right-hand image.

Note that these are the first natural cosmic-dust grains ever to be recovered from space-exposed aerogel collectors and microtomed for detailed TEM analysis. Although a very modest effort in the context of ODC, the successful recovery and subsequent TEM analysis of space-retrieved particles is significant for planetary sciences, and specifically for the in-situ characterization of comets and asteroids, the most prominent sources of interplanetary dust. Such dust is generally much more fine-grained and mineralogically diverse than typical man-made materials used in spacecraft, mandating methods more detailed and of higher spatial resolution than SEM-EDS.

Swarm Particle

2D03-22

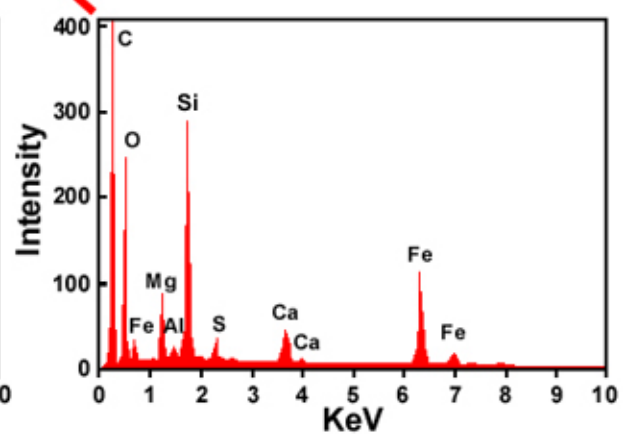
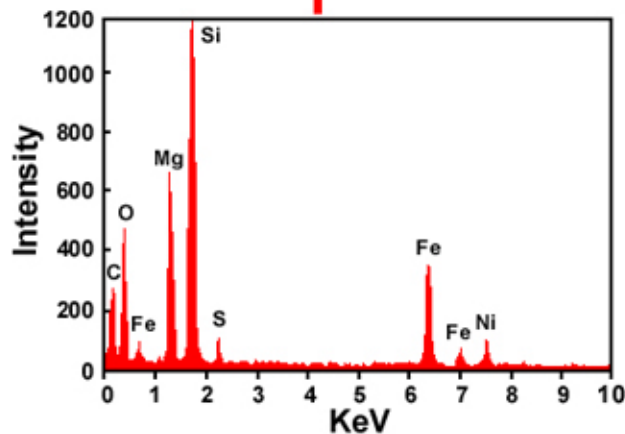
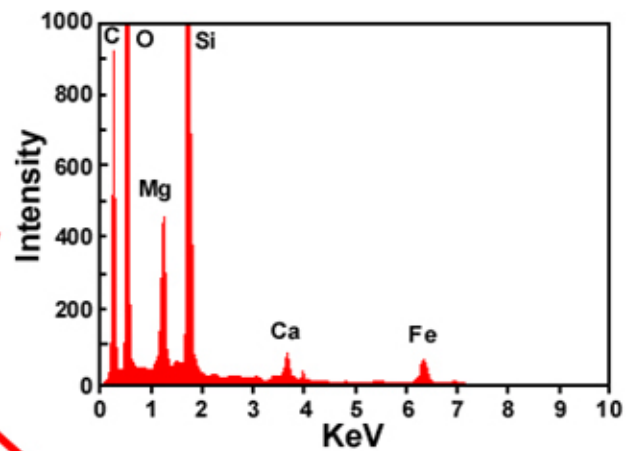
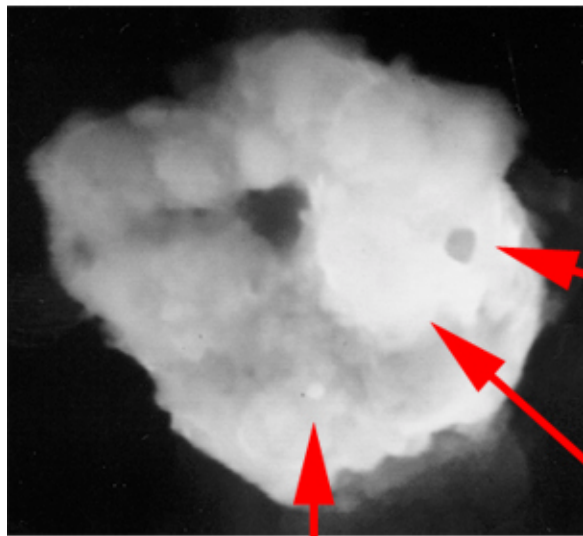


Figure 45. A particle, ~ 6 μm in size, recovered from the left track in the inserted cross section of what are obviously “swarm” tracks, all of uniform orientation. Natural particles are commonly aggregates and a number of spectra are presented to show chemical and mineralogical heterogeneity on scales of microns. Note the presence of Mg, Si, and Fe in all spectra, with Ca and S present in two, and Ni detected in only one spectrum.

Swarm Particle

2D03-29

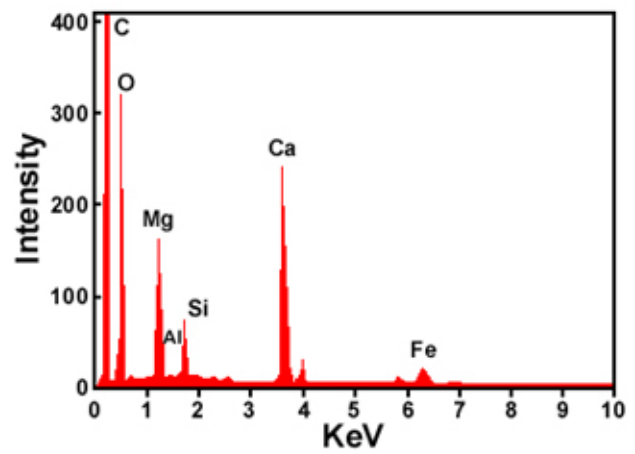
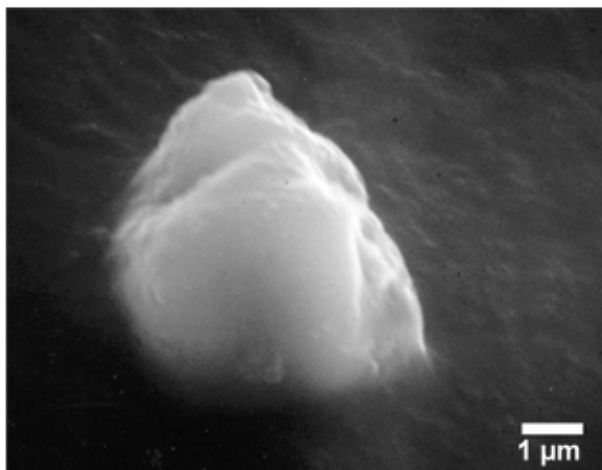
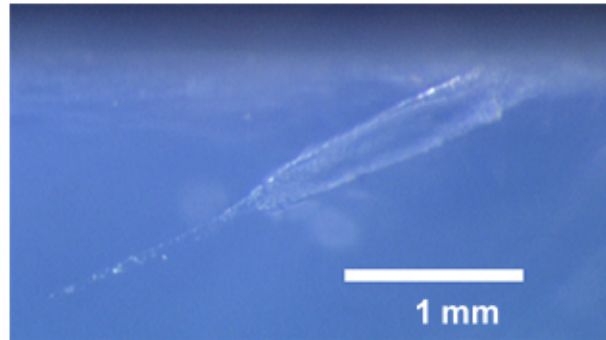


Figure 46. Another small particle recovered from the terminus of a typical swarm track ~ 500 μm in length. Note the presence of Fe, Ca, and Mg, along with modest amounts of Al and Si, typical for particles of chondritic composition. Such compositional data identifies the swarm event to be caused by a natural impactor.

Natural Particle

2D03-23

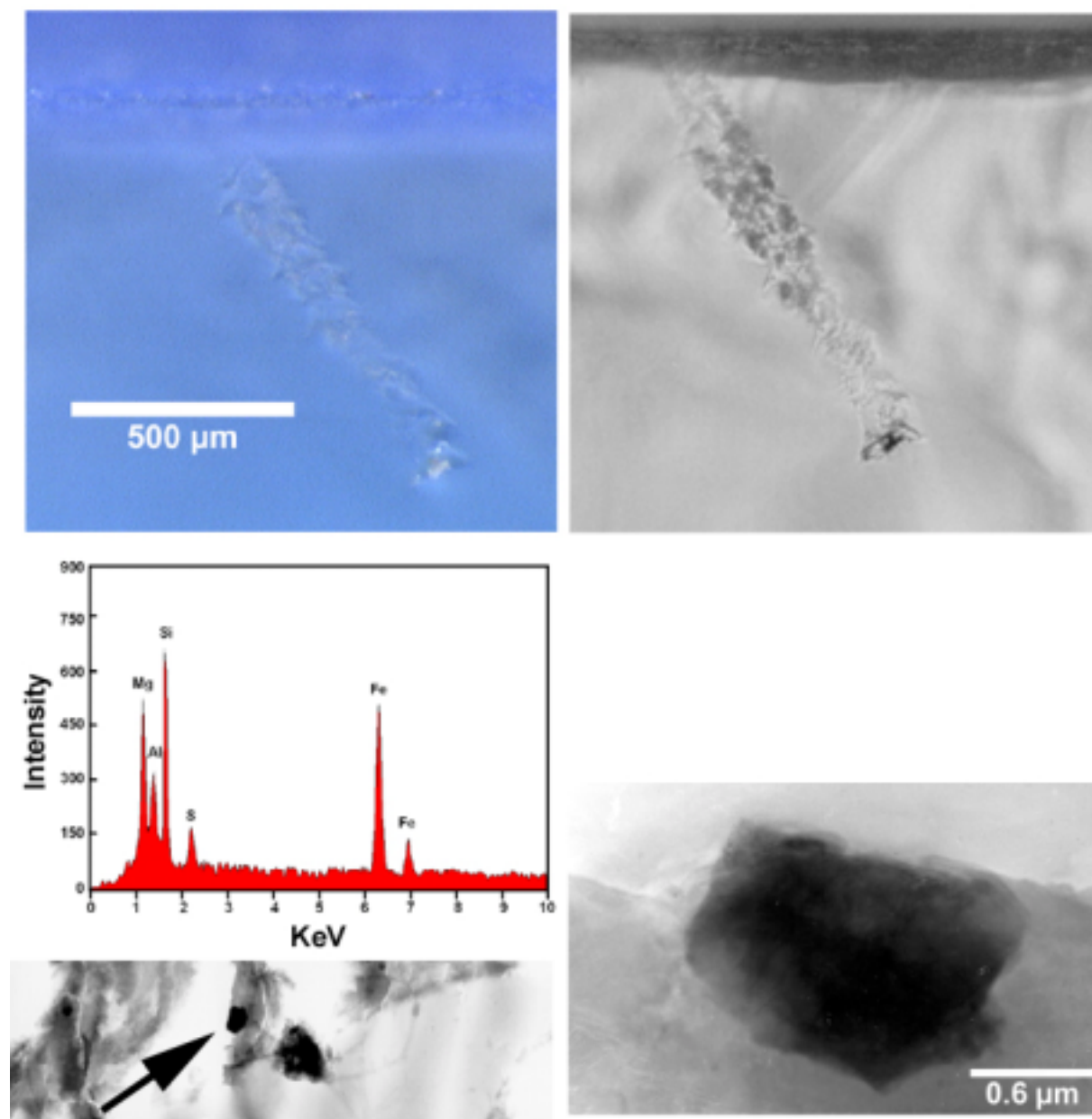


Figure 47. Natural micrometeorite particle recovered from track 2D03-23. The EDS spectrum was obtained by SEM analysis of the particle providing preliminary results that shows considerable aerogel-based Si-contamination. The sample was subsequently embedded in epoxy and thin-sectioned (*i.e.*, microtome) for detailed Transmission Electron Microscope (TEM) analysis. The TEM analyses revealed many unshocked and unmelted mineral grains throughout the projectile residue.

Natural Particle

2D03-16

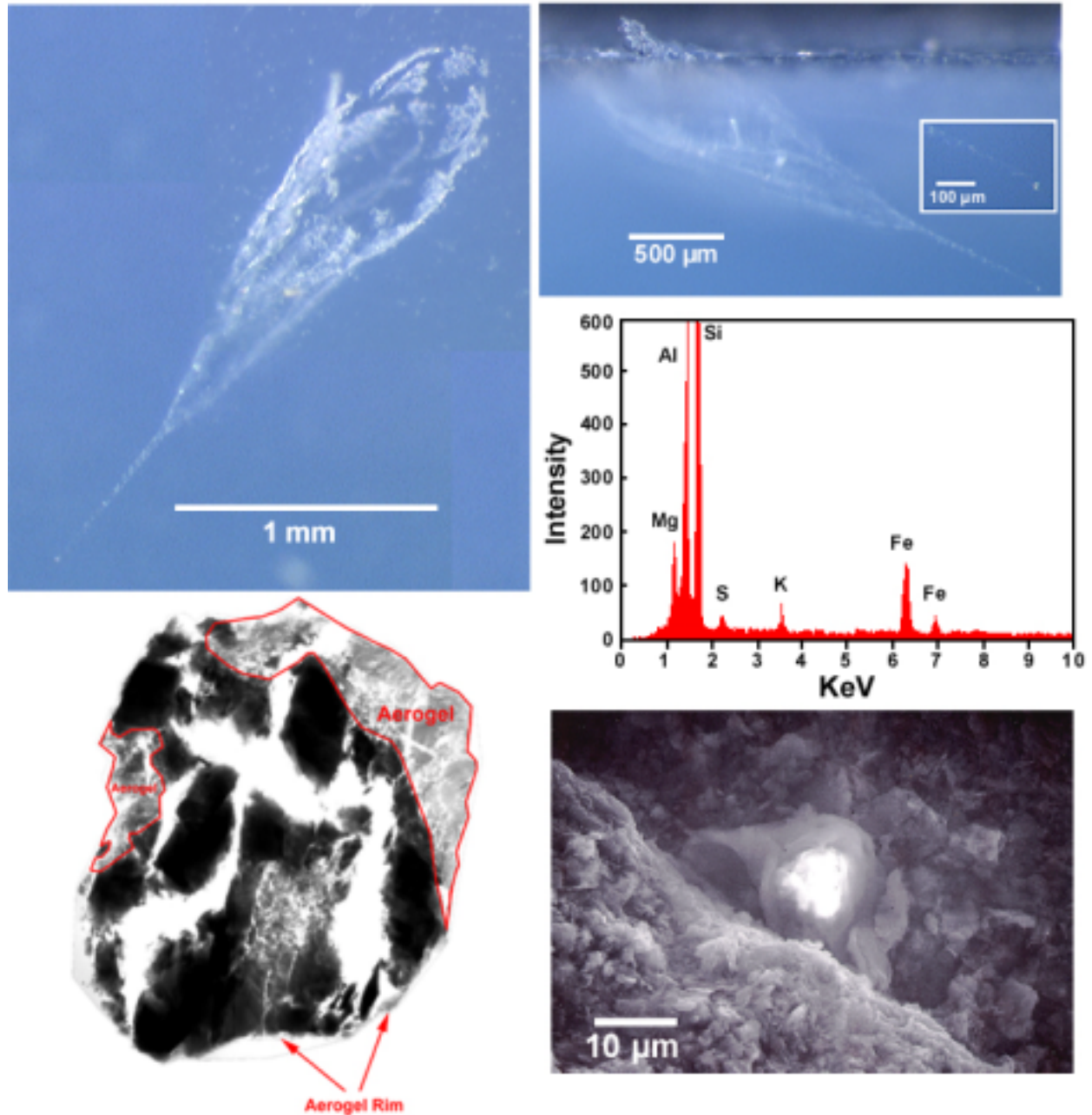


Figure 48. Example of a natural particle from track 2D03-16. The particle was removed from the aerogel host (to avoid the risk of losing a potentially valuable sample). Note that EDS spectra can be obtained from the exposed surfaces of such samples, although aerogel based Si-contamination is prevalent. The sample was subsequently embedded in epoxy and thin-sectioned via microtome for detailed Transmission Electron Microscope (TEM) analysis. The TEM image show substantial invasion of molten aerogel into the sample (white areas in left-hand figure).